

## Small-Pad Resistive Micromegas: rate capability for different spark protection resistive schemes

To cite this article: M. Iodice *et al* 2020 *JINST* **15** C09043

View the [article online](#) for updates and enhancements.



**IOP | ebooks™**

Bringing together innovative digital publishing with leading authors from the global scientific community.

Start exploring the collection—download the first chapter of every title for free.

The advertisement banner features a background of overlapping book covers with various scientific and technical illustrations. The text is presented in a clean, modern font, with the IOP logo in red and the word 'ebooks' in black with a trademark symbol. The main message is centered and easy to read.

INTERNATIONAL CONFERENCE ON INSTRUMENTATION FOR COLLIDING BEAM PHYSICS

NOVOSIBIRSK, RUSSIA

24–28 FEBRUARY, 2020

## Small-Pad Resistive Micromegas: rate capability for different spark protection resistive schemes

M. Iodice,<sup>a,1</sup> M. Alviggi,<sup>c,d</sup> M.T. Camerlingo,<sup>b,a,f</sup> V. Canale,<sup>c,d</sup> M. Della Pietra,<sup>c,d</sup>  
C. Di Donato,<sup>d,e</sup> P. Iengo,<sup>d,f</sup> F. Petrucci,<sup>b,a</sup> E. Rossi<sup>b,a</sup> and G. Sekhniaidze<sup>d</sup>

<sup>a</sup>INFN Roma Tre, Rome, Italy

<sup>b</sup>Università di Roma Tre, Rome, Italy

<sup>c</sup>Università di Napoli Federico II, Naples, Italy

<sup>d</sup>INFN Napoli, Naples, Italy

<sup>e</sup>Università di Napoli Parthenope, Naples, Italy

<sup>f</sup>European Center for Nuclear Research, CERN, Geneva, Switzerland

E-mail: [mauro.iodice@roma3.infn.it](mailto:mauro.iodice@roma3.infn.it)

**ABSTRACT:** Started few years ago, the goal of this R&D project is to develop a new generation of single amplification stage resistive MPGD based on Micromegas technology with the following characteristics: stable and efficient operation up to 10 MHz/cm<sup>2</sup> particle flows; high granularity readout with small pads of the order of mm<sup>2</sup>; reliable and cost-effective production process.

The miniaturization of the readout elements and the optimization of the spark protection system, as well as the stability and robustness under operation, are the primary challenges of the project.

Several Micromegas detectors have been built with similar anode planes, segmented with a matrix of 48×16 readout pads with a rectangular shape (0.8×2.8 mm<sup>2</sup>) and with a pitch of 1 and 3 mm in the two coordinates. The active surface is 4.8×4.8 cm<sup>2</sup> with a total number of 768 channels, routed off-detector for readout. With this anode/readout layout, the spark protection resistive layer has been realized with two different techniques: a pad-patterned embedded resistor with screen printing, and a uniform DLC (Diamond Like Carbon structure) layer by sputtering. For each technique different configurations and resistivity values have been adopted. For the DLC series, the most recently built prototype exploits the availability of copper clad DLC foils to improve the construction.

Characterization and performance studies of the detectors have been carried out by means of radioactive sources, X-Rays, and test beam. A comparison of the performance obtained with the different resistive layout and different configurations are presented, in particular focusing on the response under high irradiation and high rate exposure.

**KEYWORDS:** Gaseous detectors; Micropattern gaseous detectors (MSGC, GEM, THGEM, RETHGEM, MHSP, MICROPIC, MICROMEGAS, InGrid, etc); Particle tracking detectors (Gaseous detectors)

<sup>1</sup>Corresponding author.

---

## Contents

<b>1</b>	<b>Introduction</b>	<b>1</b>
<b>2</b>	<b>Detectors Design. Description of the different resistive schemes.</b>	<b>2</b>
2.1	The Pad-Patterned embedded resistors layout (PAD-P)	2
2.2	The DLC layout	2
2.3	The DLC improved layout with the sequential build-up technique (SBU)	3
<b>3</b>	<b>Characterization of the detectors</b>	<b>4</b>
3.1	Rate capability	4
3.2	Dependence on the exposed area	5
3.3	Test beam results	6
<b>4</b>	<b>Conclusions</b>	<b>7</b>

---

## 1 Introduction

Micromegas are single stage amplification gaseous detectors based on parallel plate electrode structure. The gas volume is divided into two gaps by means of a stainless steel micro-mesh: one gap between the mesh and the cathode plane, of a few mm (the conversion and drift gap), and the other gap between the mesh and the anode plane of about 0.1 mm (the amplification gap), with the anode hosting the read-out elements, usually micro-strips. An electric field of few hundreds V/cm is applied between the mesh and the cathode, in the drift region, while a more intense electric field with values of 40–50 kV/cm is supplied in the thin gap between the mesh and the strips (in the amplification region). For high rate applications and/or intense flow of highly ionising particles, discharges effects are greatly mitigated with the implementation of a layer of resistive strips facing the amplification gap [1]. This is, for example, the solution developed by ATLAS for operations up to few kHz/cm<sup>2</sup> [2].

The main goal of the present project is the development of resistive Micromegas detectors, aimed at stable operation under very high rates, up to 10's MHz/cm<sup>2</sup>. Among the possible applications: the ATLAS very forward extension of muon tracking (which is an option for future upgrades), as well as muon detectors or TPC at future accelerators. The basic steps to achieve this goal are: the optimisation of the spark protection resistive scheme and the miniaturization of the readout elements. In summary, the keywords of the project are:

- Rate capability up to 10's MHz/cm<sup>2</sup>;
- Low occupancy, requiring high granularity with readout elements (pixels/pads) with dimensions of few mm<sup>2</sup>;
- Spatial resolution (depending on the application) of the order of 100 μm;
- Robustness, i.e. stable operation under high ionisation, with limited spark rates, for long time.

## 2 Detectors Design. Description of the different resistive schemes.

All Small-Pad Micromegas detectors presented in this paper consist of a similar anode plane, segmented with a matrix of  $48 \times 16$  readout pads. Each pad has a rectangular shape ( $0.8 \times 2.8 \text{ mm}^2$ ) with a pitch of 1 and 3 mm in the two coordinates. The active surface is  $4.8 \times 4.8 \text{ cm}^2$  with a total number of 768 channels, routed off-detector for readout.

The layout of the anode plane can be seen in figure 1 (top-left). On top of this anode plane, two different concepts of the spark protection resistive layers have been implemented.

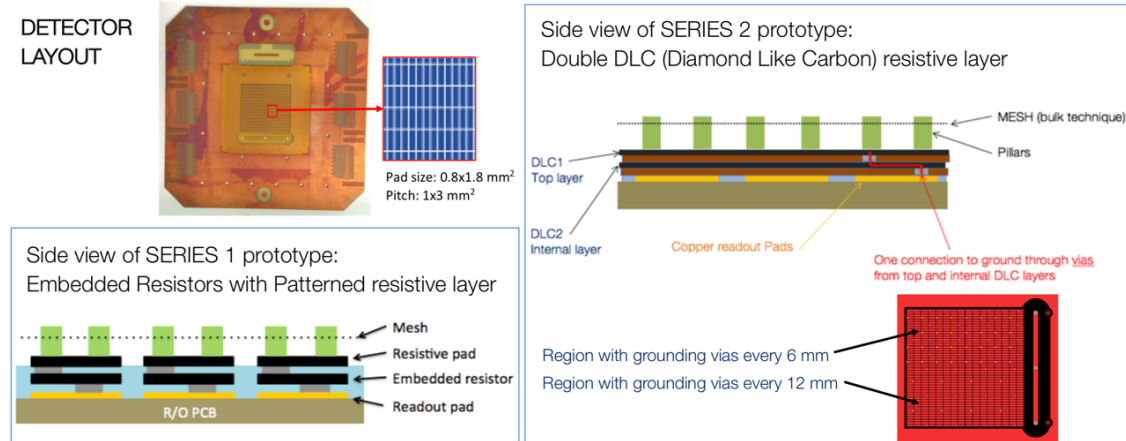


**Figure 1.** Top-left: photo of the anode plane PCB with an expanded view of the pad structure; bottom-left: side view sketch of the pad-patterned resistive scheme; right: side view sketch of the DLC detectors with a top view of the grounding vias layout. The drift gap and cathode plane are not shown in the sketches. Dimensions are not to scale.

### 2.1 The Pad-Patterned embedded resistors layout (PAD-P)

The first solution adopts a pad-patterned resistive scheme [3–5]. It relies on the anode pads being overlaid by resistive pads, interconnected by intermediate “embedded” resistors, as shown in figure 1 (bottom-left). The total resistance between the resistive and anode pads is in the range 3–7 M $\Omega$ . The main characteristic of this detector, different from the other schemes, is that each pad is totally separated from the others, for the anode, as well as for the resistive part. In the following, we will refer to PAD-P for the detector built with the pad-patterned technique.

It should be noted that a double layer of resistors, with staggered connection vias, is necessary to guarantee an almost uniform resistance to the anodic pads, independent of the impact position of the electron avalanche. With a single layer, avalanches close to vias would experience very low resistance.

### 2.2 The DLC layout

The second scheme uses two continuous resistive layers of Diamond Like Carbon structures (DLC), deposited by sputtering on kapton foils and glued on the anode. The two resistive layers are interconnected with the readout pads with a network of conducting vias (filled with silver paste) with

a few mm pitch to evacuate the charge, as sketched on figure 1 (right). Actually, the detector active plane was divided in two halves, each one having a different pitch of the conducting vias through the DLC layers: 6 mm and 12 mm respectively (also shown in the figure). The spark protection mechanism with a double DLC layer was inspired by the technique used for the development of  $\mu$ -RWELL detectors prototypes [6]. Two detectors have been built with the standard DLC technique with different resistivity: the first one with resistivity in the range 50–70  $M\Omega/\square$ , and the other with foils with about 20  $M\Omega/\square$ , referred to as **DLC50** and **DLC20**, respectively. In order to distinguish the two regions with 6 mm and 12 mm vias pitch, the suffixes “6-mm” and “12-mm” are added to the corresponding name.

### 2.3 The DLC improved layout with the sequential build-up technique (SBU)

For the latest built prototypes, the availability of copper clad DLC foils has been exploited to improve the construction technique, making use of the “sequential build up” (SBU) process [7]. The first advantage of this technique is that it allows to use the photolithographic process (applied after removing the copper everywhere except at the vias positions) to precisely locate the conductive vias and align them below the pillars. This prevents sparks in those regions where the conductive vias can be misplaced and partially exposed to the gas gap. The second advantage is that this technique is fully compatible with standard PCB processes, significantly facilitating the technological transfer of the production. In figure 2 the basic steps of the SBU construction are described, and an example of a mis-aligned vias in the standard DLC is shown as compared with the pattern that can be realised with the SBU technique.

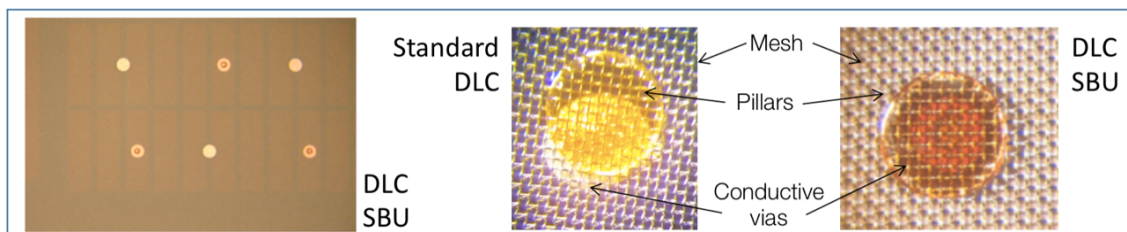


**Figure 2.** Left: top view of a small portion of the anode plane of a SBU prototype, after gluing of the first DLC layer, covering the readout pads (that can be seen in transparency). The copper circles to produce the conductive vias are visible. The smaller circles in some of them are the conductive vias between this DLC layer and the underlying pads; the “plain” copper circles will then host the staggered connections between this DLC layer and the top one, facing the gas gap. Centre: example of pillar (uppermost yellow circle) in DLC20/50 prototypes, not well centred with the conductive vias. The mesh layer can also be seen. Right: example of well centred pillar in SBU prototypes.

Two prototypes have been built with the SBU technique, referred to as **SBU1** and **SBU2**. In both cases, the configuration with the 6 mm pitch grounding vias is adopted in the full area. Both detectors were built with a 35  $M\Omega/\square$  bottom resistive layer (closest to the anode pads) and with a top layer (in the gas-gap region) with 5  $M\Omega/\square$  resistivity, lower than the requested one ( $\sim 20 M\Omega/\square$ ).

### 3 Characterization of the detectors

All the detectors have been characterised with measurements with radioactive sources ( $^{55}\text{Fe}$ ), and with 8 keV photons from a Cu X-rays gun at the GDD Lab at CERN. They were operated with the ageing-free gas mixture  $\text{Ar}/\text{CO}_2 = 93/7$ , with a nominal setting of 300 V across the 5 mm drift gap. A review of the results obtained with the detector using the pad-patterned resistive layer (PAD-P) can be found in [6]. In summary, the main characteristics of this detector are the following: it is a very robust detector without any indication of early onset of discharges for gains up to few  $10^4$ ; the energy resolution is modest (as measured with  $^{55}\text{Fe}$ ) in the range of 40–50% FWHM; the spatial resolution in the precision coordinate (1 mm pitch of the pads) is about  $190\ \mu\text{m}$ . It has a very good rate capability, up to X-rays irradiation with photon conversion rates as high as  $100\ \text{MHz}/\text{cm}^2$ , which will be quantitatively compared with the other detectors in the next sections, with new data. Preliminary studies on DLC detectors, in comparison with the PAD-P results have been published in [8] and are under publication in [9, 10]. We have reported that the energy resolution has been significantly improved with the DLC scheme ( $\text{FWHM} < 30\%$ ) and that there are no visible effects of charging-up.

#### 3.1 Rate capability

The gain of the PAD-P and DLC-20 detectors in the range of rates up to  $30\ \text{MHz}/\text{cm}^2$ , is reported in figure 3, for different values of the amplification voltage, as measured with X-rays. PAD-P shows a significant gain drop at “low” rates dominated by charging-up effect of the dielectric (Kapton) around the pads, up to about 20% at  $20\ \text{MHz}/\text{cm}^2$  at 530 V, while it has a negligible ohmic voltage drop for the individual pads in this range of rates. The DLC-20 detector shows a significant ohmic voltage drop for rates higher than a few  $\text{MHz}/\text{cm}^2$  (with a relative drop of about 20% at  $20\ \text{MHz}/\text{cm}^2$  at 510 V). It has also been observed that all the DLC series detectors, including the SBU type, have approximately the same gain behaviour, and show systematically a gain higher than PAD-P (at low/moderate rates) for the same value of the amplification voltage owing to the less uniform electric field in the amplification gap of the PAD-P prototype, where significant pad-edge effects occur (also being responsible of the worse energy resolution as compared with the DLC). In order to compare results on the rate capabilities among the different detectors, we have operated them at

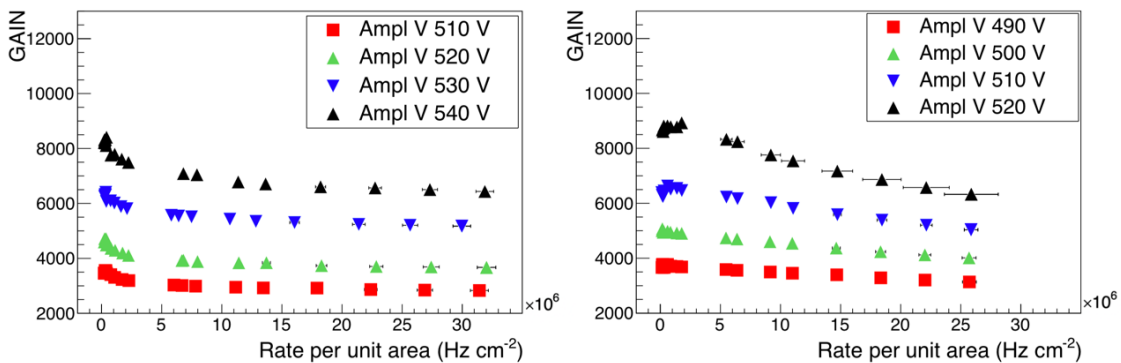


**Figure 3.** Measurements of the gain of the prototypes PAD-P (left) and DLC-20-6mm (right) in the range of rates up to  $30\ \text{MHz}/\text{cm}^2$  for different values of the amplification voltage, as measured with X-rays.

approximately the same gain (at low rates), around 6500, setting the reference operating conditions at 530 V for the amplification voltage of PAD-P and 510 V for all DLC types.

In figure 4, the dependence of the gains of the PAD-P, DLC and SBU detectors, normalised to their value at low rates, are reported as a function of the hit rates, in the range 1–100 MHz/cm<sup>2</sup>. Data are taken with a shielding defining an almost uniform irradiated area in a circle of 1 cm (0.79 cm<sup>2</sup>). In the comparison between the different detectors, the following conclusions can be drawn: PAD-P has a very different behaviour from all the DLC types. Its gain drop is dominated by the charging up, increasing with the rates, which almost saturates around 20 MHz/cm<sup>2</sup> where the gain drops by about 20%. The voltage ohmic drop is contributing only for very high rates (with currents larger than  $\sim 0.5 \mu\text{A}$  per pad) up to a total gain drop of about 30% at 100 MHz/cm<sup>2</sup>. In the comparison between the different DLC configurations, at rates above 10 MHz/cm<sup>2</sup>, the DLC-50 prototype is more severely affected by the ohmic voltage drop and the gain is significantly reduced, as expected due to its higher resistivity. It can also be seen that the configuration with 6 mm pitch grounding vias gives better performance. For what concerns the DLC20-6mm and SBU2 detectors, they show a similar behaviour at high rates, with a gain drop similar to PAD-P at about 20 MHz/cm<sup>2</sup>, further reduced up to about 50% at 100 MHz/cm<sup>2</sup>.

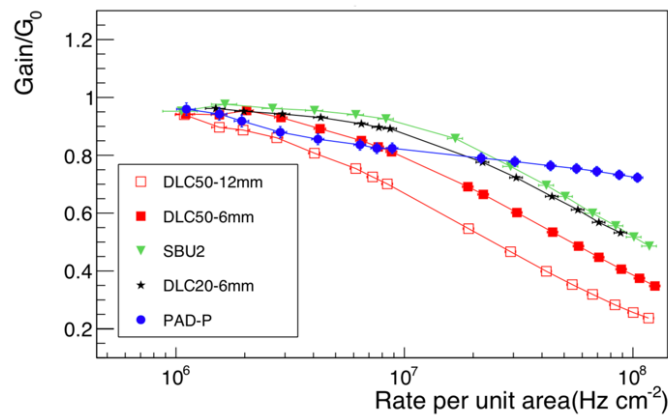


**Figure 4.** Dependence of the gains of the PAD-P, DLC and SBU detectors, normalised to their value at low rates, as a function of the X-Rays hit rates, in the range 1–100 MHz/cm<sup>2</sup>. The detectors were irradiated in a circular area of 1 cm diameter (0.79 cm<sup>2</sup>). The amplification voltage was set to have a gain about 6500 at 100 kHz/cm<sup>2</sup> for all the detectors

### 3.2 Dependence on the exposed area

All the measurements shown so far are related to an X-rays exposed surface of 0.79 cm<sup>2</sup>. In order to study the dependence of the detector's response on the irradiated area, shields with different apertures have been used. In figure 5 the gain normalised to its value at low rate for each prototype, for PAD-P (left) and DLC-20-6mm (right) is reported as a function of the rate and for three different shielding shapes: the circle of 1 cm diameter (0.79 cm<sup>2</sup>), two squares with sides 1.92 cm (3.69 cm<sup>2</sup>) and 3 cm (9 cm<sup>2</sup>). While PAD-P, thanks to its structure with independent pads, doesn't show any significant dependence on the irradiated area, in the DLC prototype there is a significant further drop in gain above few tens MHz/cm<sup>2</sup> for larger exposed surfaces with respect to the measurements

with the aperture of  $0.79 \text{ cm}^2$ . It must be noted that the drop saturates for areas larger than  $3.69 \text{ cm}^2$ . This is indeed an expected result when the exposed area is (much) larger than the “cell” enclosed within the grounding vias network ( $0.6 \times 0.6 \text{ cm}^2$ ). It must be remarked however, that the maximum drop observed for DLC-20 at  $20 \text{ MHz/cm}^2$  is still limited to 30%.

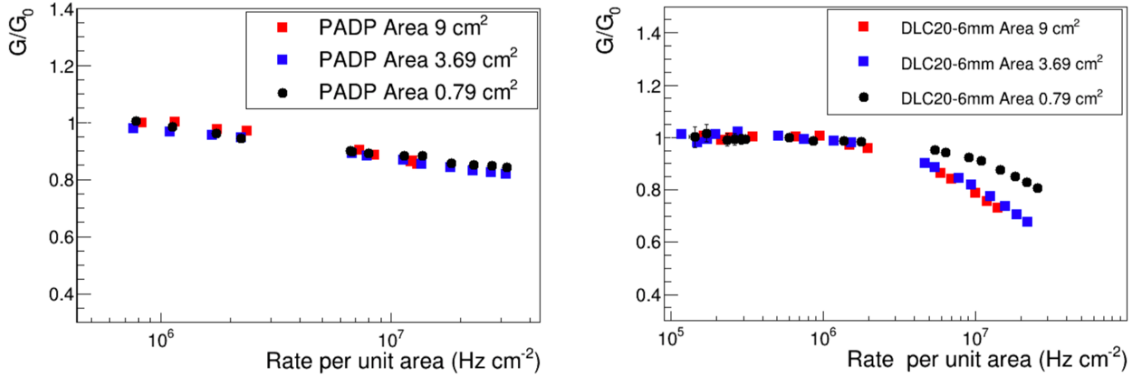


**Figure 5.** Dependence of the relative gain on the X-Rays hit rates for the PAD-P (left) and DLC-20-6mm (right) detectors for three different areas of exposure:  $0.79, 3.69, 9 \text{ cm}^2$

### 3.3 Test beam results

The performances of the detectors have been studied with  $180 \text{ GeV/c}$  muons/pions beams at CERN and, in November 2019, with a high intensity ( $\mathcal{O}(\text{MHz})$ )  $\sim 350 \text{ MeV/c}$  pion beam, at PSI.

In figure 6 the main results obtained at the test-beam at CERN are reported, comparing the prototypes PAD-P, DLC-20 and DLC-50. The left panel shows the cluster size for the three detectors, as a function of the amplification voltage. The cluster size is higher for the detectors with uniform resistive layers and increases for lower resistivity. In the right panel the spatial resolution along the precision coordinate ( $1 \text{ mm}$  pad pitch) is reported as a function of the amplification voltage. The homogeneity of the resistive layers, along with the higher cluster size, give a better resolution with

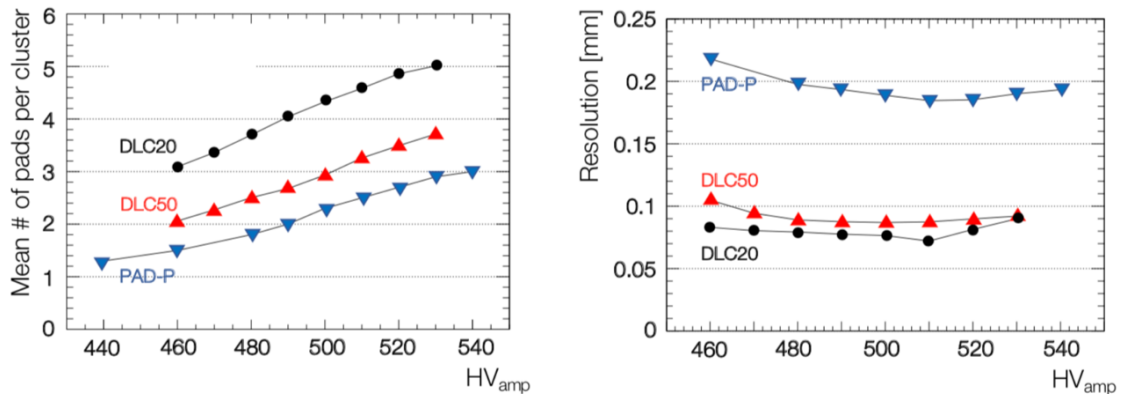


**Figure 6.** Comparison of the CERN test beam results for PAD-P, DLC20 and DLC50. Cluster size (left) and spatial resolution (right) as a function of the amplification voltage.

respect to the pad-patterned detector. For both DLC20 and DLC50 the resolution is below  $100\ \mu\text{m}$ . DLC20 reaches  $80\ \mu\text{m}$  resolution (10–20% better than DLC50) with a higher cluster size.

The main purpose of the test beam at PSI was the study of the stability of the detectors under high intensity low energy pion beams. The actual conditions of the test, however, could not allow us to test the detector at rates higher than  $5\ \text{MHz}$  on the full surface (corresponding to a density of about  $220\ \text{kHz}/\text{cm}^2$ ). This was due to logistic issues, for which our test chambers were placed downstream where the beam particle density significantly decreases. We could however collect a significant set of data, most of them currently under analysis. In figure 7 the preliminary results on the part of the tests dedicated to the study of the spark behaviour of the PAD-P, DLC and SBU detectors are reported. In the left panel, the detector currents are reported under a particle flow of about  $100\ \text{kHz}/\text{cm}^2$ , as a function of time. Some sparks can be clearly seen. Adopting the convention to count a spark at each increase of current above 30% of its average value in stable condition, we could evaluate the spark probability per hadron per  $\text{cm}^2$ . The results are reported in figure 7 right panel. PAD-P confirms its very high stability with a spark probability  $< 2 \times 10^{-9}/\text{pion}/\text{cm}^2$ . DLC20 is the most robust among the DLC series, despite the constructive improvement implemented in the construction of the SBU detectors. We explain the worse stability of the SBU detectors with the low resistivity of the top DLC layer used for their production ( $5\ \text{M}\Omega/\square$  instead of the required  $20\ \text{M}\Omega/\square$ ) that prevented us to properly assess the limits of robustness under very high rates. The SBU detectors were however operated successfully up to a maximum gain of about  $10^4$ .

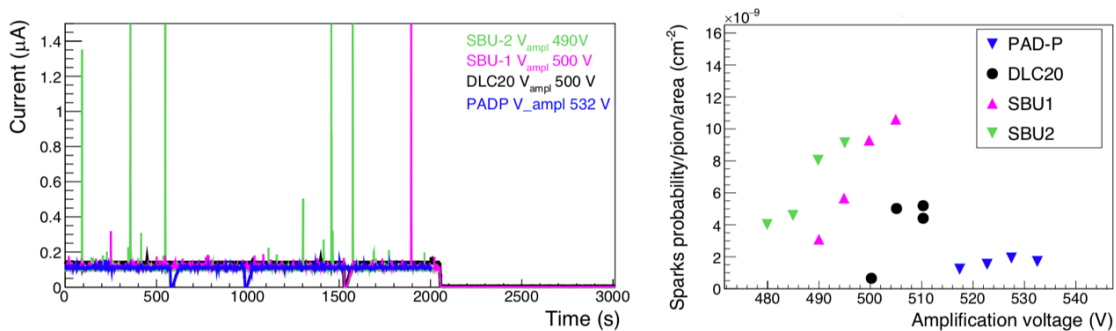


**Figure 7.** Test on detector stability at PSI with a pion beam of  $350\ \text{MeV}/c$ . Left: detector current as a function of time under a particle rate of about  $100\ \text{kHz}/\text{cm}^2$ ; right: spark probability density per pion.

## 4 Conclusions

Several small pad Micromegas detectors have been constructed implementing different resistive spark protection schemes. Their performance have been compared in similar conditions: the Ar/CO<sub>2</sub> gas mixture (with proportion 93/7) was chosen to be on the safe side to minimise ageing effects (it is possibly not the best choice and can be optimised); the reference gain of the detectors was in the range  $6500\text{--}7000$  (a quite high gain considering that most of the tests were done with X-rays inducing a ionisation much higher than minimum ionising particles — about a factor 6).

The Pad-patterned detector (PAD-P) shows a quite significant charging-up for rates higher than  $\sim 100\ \text{kHz}/\text{cm}^2$  that nevertheless saturate at  $O(1\ \text{MHz}/\text{cm}^2)$  with a gain drop of about 20%

at 20 MHz/cm<sup>2</sup>. Its gain drop is limited to  $\sim 30\%$  at a rate up to 100 MHz/cm<sup>2</sup>. It shows no dependence on the irradiated area. It can be operated in very stable conditions up to gains larger than 10<sup>4</sup>. It shows degraded performance on energy and spatial resolution compared to the detectors implementing DLC based resistive scheme. Among the latter, best performance has been obtained with the “low resistivity” DLC ( $\sim 20 \text{ M}\Omega/\square$ ) and its improved variant (SBU) in both cases considering the fine network layout of grounding vias (6 mm pitch). For these detectors the gain reduction with rates is dominated by ohmic voltage drop, with a reduction  $\sim 20\%$  at 20 MHz/cm<sup>2</sup> (as for PAD-P) when irradiated on a 1 cm spot. It drops further to about 50% at 100 MHz/cm<sup>2</sup>. The gain drop also depends on the irradiated area with an effect that saturates for surfaces larger than few cm<sup>2</sup>. The DLC series have shown excellent performance in terms of energy and spatial resolutions. Their stability and robustness of operation (in particular under high rates) is not yet at the level of PAD-P. The DLC-SBU technique is promising but not yet conclusive.

## Acknowledgments

We would like to thank the CERN MPT workshop (in particular R. de Oliveira and his group, for ideas, discussions and the construction of the detectors), E. Oliveri and the whole RD51 Collaboration for support with the tests at the Gas Detector Development (GDD) Laboratory and for the test-beam at CERN and the team of the piM1 Beam facility for their support for the test beam at PSI.

## References

- [1] T. Alexopoulos, J. Burnens, R. de Oliveira, G. Glonti, O. Pizzirusso, V. Polychronakos et al., *A spark-resistant bulk-Micromegas chamber for high-rate applications*, *Nucl. Instrum. Meth. A* **640** (2011) 110.
- [2] T. Kawamoto, S. Vlachos, L. Pontecorvo, J. Dubbert, G. Mikenberg, P. Iengo et al., *New Small Wheel Technical Design Report*, Tech. Rep., [CERN-LHCC-2013-006](#), ATLAS-TDR-020 (2013).
- [3] F. Thibaud et al., *Performance of large pixelised Micromegas detectors in the COMPASS environment*, *2014 JINST* **9** C02005.
- [4] M. Chefdeville, Y. Karyotakis, T. Geralis and M. Titov, *Resistive Micromegas for sampling calorimetry, a study of charge-up effects*, *Nucl. Instrum. Meth. A* **824** (2016) 510.
- [5] M. Alviggi et al., *Construction and test of a small-pad resistive Micromegas prototype*, *2018 JINST* **13** P11019.
- [6] G. Bencivenni et al., *The  $\mu$ -RWELL detector*, *2017 JINST* **12** C06027.
- [7] R. De Oliveira, *Study of resistive materials for MPGD protection*, in proceedings of *International Conference on Instrumentation for Colliding Beam Physics*, Novosibirsk, Russia, 24–28 February 2020.
- [8] M. Alviggi et al., *Small-pad resistive Micromegas for high rate environment: Performance of different resistive protection concepts*, *Nucl. Instrum. Meth. A* **936** (2019) 408.
- [9] M. Alviggi, M.T. Camerlingo, V. Canale, M. Pietra, C. Donato, P. Iengo et al., *Pixelated resistive bulk Micromegas for tracking systems in high rate environment*, *2020 JINST* **15** C06035.
- [10] M. Iodice, M. Alviggi, M.T. Camerlingo, V. Canale, M. Della Pietra, C. Di Donato et al., *Small-pad Resistive Micromegas: Comparison of patterned embedded resistors and DLC based spark protection systems*, *J. Phys. Conf. Ser.* **1498** (2020) 012028.